QIBA Profile:

Atherosclerosis Biomarkers by Computed Tomography Angiography (CTA)

Edition: 2023
Stage: Clinically Feasible

When referencing this document, please use the following format:

QIBA Atherosclerosis Biomarkers by Computed Tomography (CTA) 2023, Clinically Feasible. Quantitative Imaging Biomarkers Alliance, March 28, 2023. Available at: https://qibawiki.rsna.org/index.php/Profiles

Table of Contents

1. Executive Summary

The clinical application of Computed Tomography Angiography (CTA) is widely available as a technique to optimize the therapeutic approach to treating vascular disease. Evaluation of atherosclerotic arterial plaque characteristics is currently based on qualitative biomarkers. However, the reproducibility of such findings has historically been limited even among experts (1).

Quantitative imaging biomarkers have been shown to have additive value above traditional qualitative imaging metrics and clinical risk scores regarding patient outcomes (2). However, many definitions and cut-offs are present in the current literature; therefore, standardization of quantitative evaluation of CTA datasets is needed before becoming a valuable tool in daily clinical practice. To establish these biomarkers in clinical practice, techniques are required to standardize quantitative imaging across different manufacturers with cross-calibration. Moreover, the post-processing of atherosclerotic plaque segmentation needs to be optimized and standardized.

The goal of a *Quantitative Imaging Biomarker Alliance (QIBA)* Profile is to provide an implementation guide to generate a biomarker with an effective level of performance, mostly by reducing variability and bias in the measurement. The performance claims represent expert consensus and will be empirically demonstrated at a subsequent stage. Users of this Profile are encouraged to refer to the following site to understand the document's context: http://qibawiki.rsna.org/index.php/QIBA_Profile_Stages. All statistical performance assessments are stated in carefully considered metrics and according to strict definitions as given in (3-8), which also includes detailed, peer-reviewed rationale on the importance of adhering to such standards.

The expected performance is expressed as **Claims** (Section 1.2). To achieve those claims, **Actors** (Scanners, Reconstruction Software, Image Analysis Tools, Imaging Physicians, Physicists, and Technologists) must meet the Checklist **Requirements** (Section 3) covering Subject Handling, Image Data Acquisition, Image Data Reconstruction, Image QA, and Image Analysis.

This Profile is at the Clinically Feasible stage (qibawiki.rsna.org/index.php/QIBA_Profile_Stages) which indicate that multiple sites have **performed the profile and found it to be practical** and expect it to achieve the claimed performance.

QIBA Profiles for other CT, MRI, PET, and Ultrasound biomarkers can be found at qibawiki.rsna.org.

1.1 Clinical Context

Plaque composition is associated with the likelihood of rupture and downstream ischemic events but is presently known to be highly variable. Standardized protocols and analysis of plaque characteristics can increase the early identification of patients at increased risk for adverse events.

While the prevalence of tissues differs across arterial beds, the density distributions indicative of tissue type as used by the algorithms share common definitions. Plaque characteristics such as a large atheromatous lipid-rich core, thin fibrous cap, outward remodeling, infiltration of the plaque with macrophages and lymphocytes, and thinning of the media predispose to thrombosis in both carotid and coronary artery disease (9). These points support the conclusion that whereas the extent of the various plaque tissues differs across arterial beds, the cellular and molecular level milieu of the individual tissue types share common objective definitions across beds (10). Whereas inter-bed differences such as a thicker fibrous cap and a higher prevalence of intra-plaque hemorrhage in carotid vs. the coronaries affect the amount of these tissues (11), it does not change the nature of the tissues when they do present

clinically or via diagnostic imaging. Moreover, myocardial blood perfusion is regulated by the vasodilation of epicardial coronary arteries in response to various stimuli, such as nitrous oxide (NO), causing dynamic changes in coronary arterial tone that can lead to multifold changes in coronary blood flow. Similarly, carotid arteries are more than simple conduits supporting brain circulation; they demonstrate vasoreactive properties in response to stimuli, including shear stress changes (12). Endothelial shear stress contributes to endothelial health and a favorable vascular wall transcriptomic profile (13). Clinical studies have demonstrated that areas of low endothelial shear stress in the coronary tree are associated with atherosclerosis development and high-risk plaque features (14). Similarly, in the carotid arteries, lower wall shear stress is associated with plaque development and localization (15). Whereas the focus in this description is coronary and carotid arteries, which are supported explicitly in Profile sections, other arterial beds, such as peripheral vascular, also share common signatures, specifically at the molecular and cellular levels which may be used for tissue characterization.

Analysis of atherosclerotic plaque is conducted at two levels. Plaque morphology is represented as a set of individual measurands describing either structural anatomy or tissue characteristics. These biomarkers are then interpreted collectively to assess plaque stability phenotype. Each is described below.

All plaque morphology measurements are taken within a prescribed anatomical target comprising one or more vessels and at perpendicular cross-sections along the centerline of each vessel. Each cross-section presents a roughly circular lumen area (representing the blood channel) and an annular wall area (presenting the vessel wall, including plaque with its constituent tissues).

Table 1: Plaque Morphology Measurands Covered by this Profile

Measurand	Definition	Units
Maximum Wall Thickness	The cross-sectional thickness of a vessel wall is measured at the point of greatest wall thickness (given that the wall thickness is not uniform for each cross-section).	mm
Lumen Area	The cross-sectional area of a blood channel at a position along the vessel centerline.	mm^2
Lumen Volume	The 3D volume of the lumen, irrespective of how it is sliced	mm^3
Wall Area	The cross-sectional area of a vessel at a position along the vessel centerline minus the Lumen Area at that position.	mm^2
Plaque Volume, also known as Total Atheroma Volume (TAV)[a,b]	The 3D volume of the plaque, excluding minimally diseased tissues, irrespective of how it is sliced	mm^3
Plaque Burden, also known as Percent Atheroma Volume (PAV)[c,b]	An index is calculated as Wall Area / (Wall Area + Lumen Area) (with vasodilation)	unitless ratio
Lipid-Rich Necrotic Core (LRNC) Area	The area of the Lipid-Rich Necrotic Core (which is a pathologic retention of lipids, particularly lipoproteins, by intimal/medial cells leading to progressive cell loss, cell death, degeneration, and necrosis. LRNC is a mixture of lipid, cellular debris,	mm^2

[a] Historically the volume of undiseased walls has been seen as negligible resulting in the simplification to equate wall volume with plaque volume. At this Profile version we retain that simplification but inviting further discussion regarding the exclusion of undiseased tissue for a more specifically defined plaque volume may result in a change at the next version of the Profile as experimental standards converge.

[b] Plaque volume includes a range of tissues, including tissues other than LRNC, dense calcification, and IPH.

[c] Other normalizations may be considered at later stages of this Profile.

	blood, and water in various concentrations).	
LRNC Volume	The 3D volume of LRNC, irrespective of how it is sliced	mm^3
Intra-plaque Hemorrhage (IPH) Area	The area of presence of an accumulation of erythrocytes of the plaque, with or without communication to the lumen or neovasculature.	mm^2
IPH Volume	The 3D volume of IPH, irrespective of how it is sliced	mm^3
Calcified Area	The area that has been calcified (due to the physiologic defensive biological process of attempting to stabilize plaque, which has a mechanism akin to bone formation).	mm^2
Calcified Volume	The 3D volume of calcified tissue, irrespective of how it is sliced	mm^3

Arterial plaque volume and the volume of the specific tissue types are recognized key features and are a focus of this Profile (Table 1). It is noted, however, that validation of 3D volume measurements is currently difficult, as the extraction of volume information from histology specimens for ground truth is technically challenging, and this is exacerbated by the large number of specimens that would be needed to have statistical significance of the bias estimates. As a result, the performance requirements and assessment procedures are currently defined at the cross-section level, which is not to indicate the greater importance of area measurements but which already at this level represents a significant advancement in the field were at least these measurements to be rigorously validated as we indicate here. We reason that volumetry will also benefit from this validation, and, provided that image analysis software meet the qualitative requirements of using fully resolved 3D objects rather than simplifying assumptions such as the multiplication of areas by slice thickness to obtain volumes, that this Profile will also make a specific contribution to our intended purpose, namely, that both volumes as well as cross-sectional areas are essential.

Also considered important for development of the field are objective measures of Perivascular (pericoronary) Adipose Tissue in Système International (SI) units rather than arbitrary or uncalibrated scores or indices. Claims for this will be added as data allows.

Additionally, this Profile supports an objectively defined plaque stability phenotype from CTA (16).[d] The plaque phenotype classification system approved by the American Heart Association (AHA) to inform practicing clinicians on the plaque's current presentation is tied to severity levels regarding propensity to rupture. Stary's initial system (19) has been updated and refined recently (20, 21). The granularity from the histological truth basis to the CTA application is reduced to strike an optimal balance between feature visibility in radiology and the clinical utility of the classification (Table 2).

[d] Here we acknowledge related work under the broad heading "radiomics" (17. Wang X, Pennello G, deSouza NM, Huang EP, Buckler AJ, Barnhart HX, Delfino JG, Raunig DL, Wang L, Guimaraes AR, Hall TJ, Obuchowski NA. Multiparametric Data-driven Imaging Markers: Guidelines for Development, Application and Reporting of Model Outputs in Radiomics. Acad Radiol 2022. doi: 10.1016/j.acra.2022.10.001 e.g., 18. Kolossváry M, Karády J, Kikuchi Y, Ivanov A, Schlett CL, Lu MT, Foldyna B, Merkely B, Aerts HJ, Hoffmann U, Maurovich-Horvat P. Radiomics versus Visual and Histogram-based Assessment to Identify Atheromatous Lesions at Coronary CT Angiography: An ex Vivo Study. Radiology 2019;293(1):89-96. doi: 10.1148/radiol.2019190407). Compared with Quantitative Imaging Biomarkers that have an objective truth basis, radiomics extracts a large number of features from radiographic medical images using data-driven algorithms evident as patterns irrespective of ground truth basis. Clarification of terms has converged to referring to the radiomic features as data-driven imaging markers (DIMs) but lacking formal validation as required by this Profile.

Table 2: Plaque Stability Phenotype Definitions and Truth Basis

Plaque Stability Phenotype	Type at Microscopy	Other terms for same lesions
Minimal Disease	Intimal Xanthoma or Thickening	Fatty dot or streak, early lesion
Stable Plaque	Pathological Intimal Thickening, Nodular calcification, Fibro-Calcific Plaque, or Fibroatheroma	Calcified plaque, Fibrous plaque
Unstable Plaque	Ulceration, IPH, TCFA, Rupture, or Calcified Nodule (thrombus)	Atheromatous plaque, Fibrolipid plaque, Complicated lesion

When a given section presents with multiple types, only the most clinically significant type shall be annotated. The classes used maximize the value of in vivo radiology relative to the clinical utility by identifying what a pathologist would say were they to have the tissue at microscopy but doing so without tissue. From a mathematical point of view, phenotype classification outputs are polychotomous multiclass outcomes (minimal disease, stable plaque, and unstable plaque) that are not constrained physiologically for a specific order of progression beyond the fact that all disease starts as minimal.

The units are the %likelihood of the section of tissue being one of the three classes. The claim is a discrimination claim stated in terms of AUROCs are defined as the given class vs. the union of the other classes. As example, the AUROC for Unstable Plaque is the ability to separate Unstable Plaque vs. not Unstable, i.e., either Minimal Disease or Stable Plaque.

Technical challenges differ across arterial beds (e.g., use of gating, vessel size, amount, and nature of motion). In general, these effects are mitigated by scan protocol, which results in approximate in-plane voxel sizes in the 0.5-0.75mm range, and the reconstruction and scan settings often resulting in through-plane resolution of coronary (the smaller vessels) are actually better than rather than inferior to, that of carotids (with the voxels often being reconstructed to be closer to isotropic in coronary and not so in the neck and larger vessels extremities). Unless explicitly noted, the specifications and requirements are the same across beds.

While accurate measurement of degree stenosis is not indicated in the Profile explicitly, the cross-sectional lumen area is included as more objective. The intention is to take it at a reference point and each cross-section. This Profile does not address whether diameter-based vs. area-based stenosis would be of higher utility clinically or the optimal placement of reference. NASCET and ECST have extensively covered the specific question of reference. QIBA's contribution is to add area measurement (rather than being limited to diameter) but leave the topic of reference for these other works.

1.2 Claims

When all relevant staff and equipment conform to this Profile*, the* following statistical performance for measurements taken *at a single encounter* may reasonably be expected[e]:

Table 3: Quantitative Claims for individual Plaque Morphology Measurands

Measurement of	Units	Range	Bias	Slope	Inter-reader SD
Lumen Area	mm^2	0.0-30.0	0±1.0	1±0.1	2.5
Wall Area	mm^2	10.0-100.0	0±1.0	1±0.1	4.0
Maximum Wall Thickness (WT)	mm	1.0-5.0	0±1.0	1±0.2	1.0
Plaque Burden (PAV)	unitless ratio	0.4-1.0	0±0.1	1±0.1	0.5
Calcified (CALC) Area	mm^2	0.0-15.0	0±0.5	1±0.1	1.5
Lipid-Rich Necrotic Core (LRNC) Area	mm^2	0.0-15.0	0±1.0	1±0.2	1.5
Intra-plaque Hemorrhage (IPH) Area[f]	mm^2	0.0-15.0	0±2.0	1±0.2	2.0

Table 4: Quantitative Claims for Multi-parametric Plaque Stability Phenotype

Classification of	Units	Agreement with Expert Pathologists
Minimal Disease	% likelihood	AUROC 0.95 [0.9, 1.0] (vs. Stable or Unstable)
Stable Plaque	% likelihood	AUROC 0.9 [0.85, 0.95] (vs. Minimal or Unstable)
Unstable Plaque	% likelihood	AUROC 0.95 [0.9, 1.0] (vs. Minimal or Stable)

The claim tables are built based on de-rating from achievable performance of at least one reference device (22, 23).

DISCUSSION

- Technical performance claims indicate the extreme of the 95% confidence interval, not (only) the point estimate. Specifically, we say that not only is a point estimate of the performance as claimed, but that we are 95% confident that it is as claimed.
- All statistical performance metrics are stated according to strict definitions as given in (24-29).
- Section 4, Assessment Procedures, identifies the data collection and analysis procedures for the assessment:
    - 95% CI Bias for structural measurands (maximum wall thickness, lumen area, wall area, and plaque burden) are assessed as described in section 4.3. Assessment Procedure: Vessel Structure Bias and Linearity, using phantoms.
    - 95% CI Bias for tissue characteristics (LRNC, IPH, and CALC) are assessed as described in section 4.4. Assessment Procedure: Tissue Characteristics Bias and Linearity, using ex vivo histology, accounting for both subjectivity due to pathologist annotation and 2D-3D spatial alignment as identified in the assessment procedure.
    - 95% CI AUROC for plaque stability phenotype (Minimal Disease, Stable Plaque, and Unstable Plaque) are assessed as described in section 4.5. Assessment Procedure: Multi-

[e] QIBA Profile Claims are developed successively through the stages of Profile development (defined at https://qibawiki.rsna.org/index.php/QIBA_Profile_Stages). The current status of this Profile is "Clinically Feasible", with multiple sites having performed the profile and found it to be practical and expect it to achieve the claimed performance. Specifically, the performance figures on which these claims are currently based on procedures defined in Section 4.

[f] Limited evidence of prevalence in coronary but included to encourage further studies.

parametric Plaque Stability Phenotype, using ex vivo histology, accounting for both subjectivity due to pathologist annotation and 2D-3D spatial alignment as identified in the assessment procedure.

- 95% CI for reader variability is assessed as inter-reader standard deviation (SD), as described in section 4.6. Assessment Procedure: Reader / Image Analysis Tool Variability, using clinical (not phantom) data sets representing the range of presentations, specifically to include multiple arterial beds (e.g., carotid and coronary).

Regarding linearity, we distinguish between (1) the assessment of linearity, or nonlinearity, for a biomarker for developing the profile claims and (2) testing the conformance of an actor or site to the assumptions underlying the claims. For #1, methods as described in (30) are applicable. Then, given this, actors with linearity requirements identified in Section 3 of this Profile verify that their results agree with the assumptions made for the claims. For this (i.e., #2), actors (only) need to verify linearity in the range included in the claims (not a full assessment of linear and nonlinear parts) and verify that the slope is in the range assumed in the claims. This simplicity is essential for the practicality of the Profile's assessment procedures.

- Use of vendor components that have only been tested over a smaller range than specified in the claim invalidates the claim outside of that range for the combined system, including all actors.
- Maximum wall thickness refers to the largest value for point-wise wall thickness within the lesion or target.

1.3 Disclaimers

Standard of Care: The requirements are defined to achieve the Claim and do not supersede proper patient management considerations. Requirements that disqualify an exam or lesion mean the performance in the Claims cannot be presumed, but does not preclude clinical use of the measurement at the discretion of the clinician.

Confirmation of Claims: The claims are informed by groundwork studies, literature review and expert consensus. The QIBA Clinical Confirmation Stage will collect data on the actual field performance and appropriate revisions will be made to the Claims and/or the details of the Profile. At that point, this caveat may be removed or re-stated. (https://qibawiki.rsna.org/index.php/QIBA_Profile_Stages)

Innovation: Profile requirements are intended to establish a baseline level of performance. Exceeding the requirements and providing higher performance or advanced capabilities is allowed and encouraged. The Profile does not limit the methods institutions and equipment suppliers use to meet the requirements.

2. Conformance

To conform to this Profile, participating Actors (staff and equipment) shall meet each requirement on their checklist in Section 3.

- Some requirements reference a specific **assessment procedure** in Section 4 that shall be used to assess conformance to that requirement. For the rest, any reasonable assessment procedure is acceptable.
- Staff must ensure requirements assigned to them are met; however, for the purpose of conforming to the profile, they may delegate a task rather than physically doing it themselves.
- Staff names represent roles in the profile, not formal job titles or certifications. E.g., Site

equipment performance requirements are assigned to the Physicist role. The role may be filled by any appropriate person: a staff physicist, a managed contractor, or a vendor provided service.

- If a QIBA Conformance Statement is available for equipment (e.g., published by a scanner vendor), a copy of that statement may be used in lieu of confirming each requirement in that equipment checklist yourself by running the necessary tests.

To make a formal claim of conformance, the organization responsible for equipment or staff shall publish a QIBA Conformance Statement.

QIBA Conformance Statements:

- shall follow the current template: (https://qibawiki.rsna.org/index.php/QIBA_Conformance_Statement_Template)
- shall include an Appendix containing details recorded by the assessor as stated in requirements or assessment procedures (e.g., acquisition parameters)
- shall describe the test data used for conformance testing or alternatively provide access to it

3. Profile Requirement Checklists

The following Checklists are the basis for conforming to this Profile (See Section 2).

Conforms (Yes/No) indicates whether conformance to the requirement has been confirmed by the assessor. When responding No, it is helpful to include notes explaining why.

3.1 Scanner and Reconstruction Software Checklist

Make/Model/Version: Assessment Date:

Parameter	Requirement	Applies to:		Conforms?
		Coronary	Carotid	
In-plane Spatial Resolution	Shall validate that the protocol achieves an f50 value that is greater than 0.35 line pairs per mm (lp/mm) for both air and soft tissue edges (31). See section 4.1. Assessment Procedure: In-plane Spatial Resolution.	Yes	Yes	
Pixel noise	Shall validate that the protocol achieves a standard deviation that is < 30HU (31). See 4.2. Assessment Procedure: Pixel noise.	Yes	Yes	
kVp	Shall be optimized based on signal characteristics for differing patient body habitus.	Yes	No	
Acquisition Protocol	Shall be capable of making validated protocols (designed and validated by the manufacturer and/or by the site) available to the technologist at scan time.	Yes	Yes	
Temporal Resolution	Shall achieve an effective rotation time of less than or equal to 400ms.	Yes	No	

3.2 Physicist Checklist

Note: The role of "Physicist" may be played by an in-house medical physicist, a physics consultant or

other staff (such as vendor service or specialists) qualified to perform the validations described.

Physicist Name: Assessment Date:

Parameter	Requirement	Applies to:		Conforms?
		Coronary	Carotid	
Acquisition Protocol	Shall prepare a protocol to meet the specifications in this table.	Yes	Yes	
Acquisition Protocol	Shall ensure technologists have been trained on the requirements of this profile.	Yes	Yes	
Nominal Tomographic Section Thickness (T)	Shall set to Less than or equal to 0.75mm for coronary exams and Less than or equal to 1.0mm for carotid exams.	Yes	No	
Total Collimation Width	Shall set to Greater than or equal to 16mm.	No	Yes	
Reconstruction Protocol	Shall prepare a protocol to meet the specifications in this table. Shall ensure technologists have been trained on the requirements of this profile.	Yes	Yes	
Reconstructed Image Thickness	Shall be less than 1mm.	Yes	Yes	
Reconstructed Image Interval	Shall set to less than or equal to the Reconstructed Image Thickness (i.e., no gap, may have overlap).	Yes	Yes	
Reconstructed In-plane Voxel Size	Shall set to cover 10x20cm with matrix size but not less than 512x512	Yes	Yes	
In-plane Spatial Resolution	Shall validate that the protocol achieves an f50 value that is Greater than 0.35 lp/mm for both air and soft tissue edges. See section 4.1. Assessment Procedure: In-plane Spatial Resolution	Yes	Yes	
Pixel noise	Shall validate that the protocol achieves a standard deviation that is < 30HU. See section 4.2. Assessment Procedure: Pixel noise	Yes	Yes	

3.3 Technologist Checklist

Technologist Name: Assessment Date:

Parameter	Requirement	Applies to:		Conforms?
		Coronary	Carotid	
Artifact Sources	Shall remove or position potential sources of artifacts (specifically including breast shields, metal-containing clothing, EKG leads, and other metal equipment) such that they will not degrade the reconstructed CT image.	Yes	Yes	
Breath hold	Shall instruct the subject in proper breath-hold and start image acquisition shortly after full inspiration, taking into account the lag time between full inspiration and diaphragmatic relaxation.	Yes	No	
Table Height & Centering	Shall adjust the table height for the mid-axillary plane to pass through the isocenter. Shall center the thorax shall be centered in the AP and L/R directions according to the following: table	Yes	No	

Parameter	Requirement	Applies to:		Conforms?
		Coronary	Carotid	
	height shall be adjusted for the mid axillary plane to pass through the isocenter and the sagittal laser line shall pass through the sternum from suprasternal notch to xiphoid process.			
Nitrates	Shall administer nitrates as prescribed, 5-7 minutes after nitro is administered.	Yes	No	
Acquisition Protocol	Shall select a protocol that has been previously prepared and validated for this purpose.	Yes	Yes	
Reconstruction Protocol	Shall select a protocol that has been previously prepared and validated for this purpose.	Yes	Yes	
ECG Gating	Shall use prospective ECG gating and consider iterative reconstruction to allow for the lowest possible radiation exposure. If the heart rate is too high, retrospective ECG gating may be required to obtain optimal images.	Yes	No	
Reconstructed Image Thickness	Shall be less than 1mm if not set in the protocol.	Yes	Yes	
Reconstructed Image Interval	Shall set to less than or equal to the Reconstructed Image Thickness (i.e., no gap, may have overlap) and, if evaluated to determine change, consistent with baseline.	Yes	Yes	

3.4 Imaging Physician Checklist

Note: The Imaging Physician is responsible for equipping the Technologist with the protocol parameters. They may choose to use a protocol provided by the scanner vendor. Working collaboratively with a physicist is recommended as some parameters are system dependent and may require special attention.

Imaging Physician Name: Assessment Date:

Parameter	Requirement	Applies to:		Conforms?
		Coronary	Carotid	
Use of intravenous contrast	Shall prescribe a contrast protocol to achieve appropriate lumen conspicuity relative to wall tissues.	Yes	Yes	
Total Collimation Width	Shall set to Greater than or equal to 18mm.	Yes	No	
Patient Motion Artifacts	Shall confirm the images containing the lesion are free from artifact due to motion.	Yes	Yes	
Physiological motion artifact (particularly cardiac)	Shall confirm the images containing the lesion are free from artifact due to motion based on visual review for blurred anatomic features.	Yes	Yes	
Artifacts	Shall confirm the images containing the lesion are free from artifacts due to dense objects, anatomic positioning (e.g., arms down at sides), or equipment issues (e.g., ring artifacts).	Yes	Yes	
Contrast	Shall confirm that the intravascular level of contrast	Yes	Yes	

Parameter	Requirement	Applies to:		Conforms?
		Coronary	Carotid	
Enhancement	enhancement, if any, is appropriate for evaluating the lesion.			
Patient Positioning Consistency	If evaluated to determine change, shall confirm that any lesion deformation due to patient positioning is consistent with baseline (e.g., lesions may deform differently if the patient is supine in one scan and prone in another).	Yes	Yes	
Scan Plane Consistency	If evaluated to determine change, shall confirm that the anatomical slice orientation (due to gantry tilt or patient head/neck repositioning) is consistent with baseline.	Yes	Yes	
Field of View	If evaluated to determine change, shall confirm that the image field of view (FOV) resulting from acquisition and reconstruction settings appears consistent with baseline.	Yes	Yes	
Pacemaker leads, stents	Shall confirm that anatomy assessed does not contain metal artifacts.	Yes	Yes	
Result Verification	Shall review and approve segmentations produced by the Image Analysis Tool.	Yes	Yes	
Multiple encounters	Shall re-process the first encounter if it was processed by a different Image Analysis Tool or Imaging Physician.	Yes	Yes	

3.5 Image Analysis Tool Checklist

Make/Model/Version: Assessment Date:

Parameter	Requirement	Applies to:		Conforms?
		Coronary	Carotid	
Vessel structure	Shall meet or exceed the specifications, when tested over range, as given in the Claims section, according to section 4.3. Assessment Procedure: Vessel Structure Bias and Linearity, noting that the complete 95% confidence intervals (not only the point estimates) shall	Yes	Yes	
Tissue Composition	Shall meet or exceed the specifications, when tested over range, as given in the Claims section, according to section 4.4. Assessment Procedure: Tissue Characteristics Bias and Linearity, noting that the full 95% confidence intervals (not only the point estimates) shall meet or exceed the indicated specifications when tested over range as given in the Claims section.	Yes	Yes	
kVp	Shall include a calibration for differing kVp values based on material response curves experimentally measured for each tissue type.	Yes	Yes	
Histology-defined High-Risk Plaque	Shall meet or exceed the specifications, when tested over range, as given in the Claims section, according to section 4.5. Assessment Procedure: Assessment Procedure: Multi-parametric Risk Phenotype, noting that the full 95% confidence intervals (not only the point estimates) shall meet or exceed the specifications given in the Claims section.	Yes	Yes	

<table>
<tr><th rowspan="2">Parameter</th><th rowspan="2">Requirement</th><th colspan="2">Applies to:</th><th>Conforms?</th></tr>
<tr><th>Coronary</th><th>Carotid</th><th></th></tr>
<tr><td>Reader variability</td><td>Shall be validated to achieve intra-reader repeatability coefficient (RC) and inter-reader reproducibility coefficient (RDC) less than the values shown in the following table. See 4.6. Assessment Procedure: Reader / Image Analysis Tool Variability, noting that the full 95% confidence intervals (not only the point estimates) shall meet or exceed following values:
<table>
<tr><th>Measurement of</th><th>Units</th><th>RC</th><th>RDC</th></tr>
<tr><td>Lumen Area</td><td>mm^2</td><td>2.5</td><td>5.0</td></tr>
<tr><td>Wall Area</td><td>mm^2</td><td>2.5</td><td>5.0</td></tr>
<tr><td>Maximum Wall Thickness (WT)</td><td>mm</td><td>0.75</td><td>1.0</td></tr>
<tr><td>Plaque Burden (PAV)</td><td>unitless ratio</td><td>0.2</td><td>0.5</td></tr>
<tr><td>Calcified (CALC) Area</td><td>mm^2</td><td>1.0</td><td>1.5</td></tr>
<tr><td>Lipid-Rich Necrotic Core (LRNC) Area</td><td>mm^2</td><td>1.0</td><td>1.5</td></tr>
<tr><td>Intra-plaque Hemorrhage (IPH) Area</td><td>mm^2</td><td>1.0</td><td>1.5</td></tr>
</table></td><td>Yes</td><td>Yes</td><td></td></tr>
<tr><td>Basis of cross-sectional area results</td><td>Shall base cross-sectional area results on obliquely-resliced orthogonal to the centerline at spacing less than or equal to 0.5mm</td><td>Yes</td><td>Yes</td><td></td></tr>
<tr><td>Basis of volume results</td><td>Shall base volume results on three-dimensional object definitions at or higher effective resolution than the minimum resolvable partial voxel achievable with smooth interpolated contours (specifically excluding methods such as determining cross-sectional areas and multiplying by the slice thickness or other approximations)</td><td>Yes</td><td>Yes</td><td></td></tr>
<tr><td>Confidence interval</td><td>Shall be able to display to the Imaging Physician, for each measurand, the range of plausible values for the given measurement stated in terms of the completed validation for the tool as a 95% interval.</td><td>Yes</td><td>Yes</td><td></td></tr>
<tr><td>Multiple Lesions</td><td>Shall allow multiple lesions to be measured.
Shall either correlate each measured lesion across encounters or support the Imaging Physician to associate them unambiguously.</td><td>Yes</td><td>Yes</td><td></td></tr>
<tr><td>Multiple encounters</td><td>Shall be able to present the reader with both encounters side-by-side for comparison when processing the second encounter.
Shall be able to re-process the first encounter (e.g., if it was processed by a different Image Analysis Tool or Imaging Physician).</td><td>Yes</td><td>Yes</td><td></td></tr>
</table>

4. Assessment Procedures

To conform to this Profile, participating staff, and equipment ("Actors") shall support each activity assigned to them in Section 3. Although most of these requirements can be assessed for conformance by direct observation, some performance-oriented requirements cannot. The requirement references that stipulate an Assessment Procedure are described here.

4.1. Assessment Procedure: In-plane Spatial Resolution

A manufacturer or an imaging site can use this procedure to assess the In-plane Spatial Resolution of reconstructed images. Resolution is evaluated in terms of the f50 value (in mm^{-1}) of the modulation transfer function (MTF).

The assessor shall first warm up the scanner's x-ray tube and perform calibration scans (often called air-calibration scans) according to scanner manufacturer recommendations. The assessor shall scan a spatial resolution phantom, such as the ACR CT Accreditation Program (CTAP) Phantom's module 1 or one of the many applicable phantoms mentioned in AAPM TG233. The phantom shall be positioned with the center of the phantom at the isocenter and aligned adequately along the z-axis. When the scan is performed, the assessor shall generate an MTF curve, measured as an average of the MTF in the x-y plane along the edge of a target soft-tissue equivalent insert using AAPM TG233 or equivalent methodology as implemented in manufacturer analysis software, AAPM TG233 software or equivalent. The assessor shall then determine and record the f50 value, defined as the spatial frequency (in mm^{-1} units) corresponding to 0.5 MTF on the MTF curve.

The assessor shall also generate the MTF curve and determine the f50 value using the edge of the "air insert" (i.e., an open cutout in the phantom). If the phantom does not have a cutout that provides an air edge to assess, it is permitted to use the edge of the phantom.

The procedure described above is provided as a reference method. This reference method and the method used by the scanner manufacturer for FDA submission of MTF values are accepted methods for this assessment procedure. Note that the manufacturer may have specific test methodologies appropriate for the iterative reconstruction algorithm.

4.2. Assessment Procedure: Pixel noise

A manufacturer or an imaging site can use this procedure to assess the pixel noise of reconstructed images. Pixel noise is evaluated in terms of the standard deviation of pixel values when imaging material with uniform density.

Scan parameters, especially current (mA) and tube potential (kVp), strongly influence pixel noise when adjusted to accommodate the patient size. The assessor shall scan a phantom of uniform density, such as the ACR CT Accreditation Program (CTAP) Phantom's module 3, which is a 20 cm diameter cylinder of water equivalent material. The phantom shall be placed at the isocenter of the scanner. When the scan is performed, the assessor shall select a single representative image from the uniformity portion of the phantom. A region of interest (ROI) of at least 400 mm^2 shall be placed near the center of the phantom. The assessor shall record the values reported for the ROI mean and standard deviation.

Note that noise is assessed here in a standard-sized object. In cases of protocols adaptive to the patient size (such as those using Automatic Exposure Control), the qualification of CT scanner noise should include noise as a function of several different sizes if there is any concern that the noise performance may be

outside compliance for different sizes.

4.3. Assessment Procedure: Vessel Structure Bias and Linearity

This procedure is intended to be done by the Image Analysis Tool vendor to assess the bias and linearity of vessel structure measurements (lumen area, wall area, maximum wall thickness, and plaque burden). The bias and linearity of vessel structure measurements are estimated using a set of phantoms where ground truth measurements assessed by micrometer are known.

4.3.1 OBTAIN TEST IMAGE SET

The test image set consists of scanned physical phantoms (Figure 4-1). The phantoms shall be fabricated according to specifications that mimic appropriate CT characteristics and in sizes that represent a range of vessel sizes and presentations of interest. The phantoms shall be filled with contrast media utilized in practice and scanned in at least three different scanner settings that meet this Profile's requirements (to account for acquisition protocol variations). Statistical measures of bias were estimated from these data.

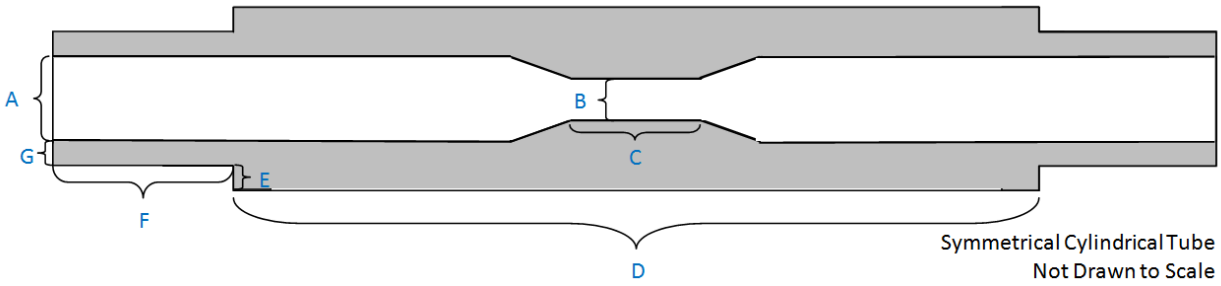

Figure 1: Physical Dimensions of Vascular Phantoms

An example material is Noryl, which has a 1.06 g/ml density. The specifications for the phantoms that shall be used are displayed in Table 5, or equivalent with scientific justification. Suppose a given Image Analysis Tool vendor wishes to support a subset of the phantoms listed rather than the whole range. In that case, a representation of conformance needs to clearly note the reduced scope (i.e., only a portion of the range indicated in the Image Analysis specification section).

Table 5. Phantom Specifications

		A		B		C			D	E	F	G
Phantom number	Surrogate artery	Reference diameter (mm)	Reference area (mm^2)	Stenosis diameter (mm)	Stenosis area (mm^2)	Stenosis length (mm)	Diameter stenosis (%)	Area stenosis (%)	Tube length1 (mm)	Tube thick1 (mm)	Tube length2 (mm)	Tube thick2 (mm)
1	coronary	2.0	3.1	0.7	0.4	10.0	65.0	87.8	40.0	1.0	80.0	1.0
2	coronary	4.0	12.6	1.3	1.3	10.0	67.5	89.4	40.0	1.0	80.0	1.0
3	coronary	4.0	12.6	2.7	5.7	10.0	32.5	54.4	40.0	1.0	80.0	1.0
4	carotid	6.0	28.3	2.0	3.1	10.0	66.7	88.9	40.0	1.0	80.0	1.0
5	carotid	6.0	28.3	3.0	7.1	20.0	50.0	75.0	80.0	1.0	60.0	1.0
6	carotid	6.0	28.3	4.0	12.6	20.0	33.3	55.6	80.0	1.0	60.0	1.0

Each tube is a surrogate for one or more blood vessels. Phantom 1, 2, and 3 represent the size range of coronary arteries. Phantom 3 represents coronary and vertebral arteries. Phantom 4, 5, and 6 represent carotid arteries. For the scans, the phantoms shall be filled with a diluted contrast agent (e.g., Omnipaque) between 10-12 mg Iodine /ml to achieve the same contrast between the vessel wall and lumen found in

patient CTA scans at 100-120 kVp (based on the published relationship of iodine concentration vs. HU for 80-120 kVp, ref. (32)).

4.3.2 DETERMINE MEASURANDS

Import the DICOM files into the analysis software, perform the analysis, and perform steps as required by the Image Analysis Tool to segment lumen and wall consistent with the requirements set in the Image Analysis activity specification. The assessor is permitted to edit the segmentation or seed point if that is part of the regular operation of the tool. Results should explicitly indicate whether they were achieved with and without editing if segmentation edits are performed. When evaluating the Image Analysis Tool, at least two readers of average capability who have been trained on the tool shall be used for this assessment procedure. When assessing an Imaging Physician, it is acceptable to use a single tool for the assessment procedure. The assessor shall calculate each cross-section's measurands (Y) (denoted Y_i), where Y denotes the measurand, and *i* denotes the *i*-th target.

4.3.3 CALCULATE STATISTICAL METRICS OF PERFORMANCE

The true measurements (X_i) as assessed by a micrometer of each cross-section are known and are provided in the dataset. The assessor shall calculate the individual percentage bias (b_i) of the measurement of each cross-section as $b_i = lnY_i - ln\ X_i$

The assessor shall estimate the population bias over the N cross-sections as $\widehat{D} = \sqrt{\sum_{i=1}^{N} b_i\ /N}$

The assessor shall convert to a percentage bias estimate as $\%\widehat{bias} = \left(\exp\left(\widehat{D}\right) - 1\right) \times 100.$

To assess linearity, the assessor shall use the NCCLS approach, EP06-A "Evaluation of the linearity of quantitative measurement procedures: A statistical approach; Approved Guideline (2003), of fitting first, second, and third order polynomials and testing that the nonlinear coefficients are near zero. Then estimate the linear slope and provide a 95% CI. The assessor is also recommended to plot the measurand estimate ($\ln Y_i$ versus $\ln X_i$) and record the OLS regression curve of the estimates as part of the assessment record.

4.4. Assessment Procedure: Tissue Characteristics Bias and Linearity

This procedure is intended to be done by the Image Analysis Tool vendor to assess the bias and linearity with which tissue characteristics are measured. Histopathology is used as ground truth.

4.4.1 OBTAIN TEST IMAGE SET

Perform histology processing and assessment only at accredited centers and ensure that ground truth processing is blinded to all other study data. Ground truth is defined as 2-dimensional annotations for each tissue type on at least 90 sections from excised tissue samples from at least 18 subjects spaced at least 2 mm apart (or equivalent number from larger number of subjects taking into account inter-section correlations from a given subject) by board-certified pathologists collected from at least two different clinical centers. These are then positioned within the 3-dimensional CTA volume blinded to any results of the Image Analysis Tool. Regarding the sample size considerations, a given tool may require a larger number of sections or specimens to characterize the performance properly. Results from this assessment procedure may be applied across arterial beds, provided that the source of tissue samples is explicitly indicated in the conformance statement.

Process sections at 2.0 mm throughout the length of the tissue specimen. It is acceptable to exclude sections (within reason and in no event cherry-picking desirable sections) when the sample is too distorted, if it is missing significant portions due to specimen processing, if there are not enough visible tissue characteristics or distinct morphology to orient the *ex vivo* histology image to the *in vivo* radiology imaging, or if the pathologist marked tissue as a mixture of tissue types.

Correlate histology cross-sections with locations in the CT image volume. In one acceptable method:

- Tissue portions of histopathologic images are converted into a mesh to facilitate returning its shape to its *in vivo* original using a finite element method (FEM) that factors in the tissue material type to simulate the stretching/compression of the relatively elastic material, and then
- Allow a positioner to rotate, tilt, and move the histology cross-section in 3D to provide a plausible alignment between the histopathology and radiology presentation.

It is important to note that the matching shall be performed using only primary CT images, scrupulously avoiding the use of the Image Analysis Tool's computed segmentations to preserve objectivity in the matching.

The subjectivity of 3D placement shall be systematically mitigated with consideration due to the sources of potential misalignment: (a) longitudinal displacement up or down the length of the vessel, (b) the angular tilt of the plane away from perpendicular to the vessel, and (c) the angular spin about the vessel.

Sample Size Considerations: Determination of the number of specimens and sections depends on the performance of the image analysis tool. The width of 95% confidence intervals for the bias and the between-subject variance as a function of sample size according to the following assumptions were made:

1) the cross-sectional area calculations are normally distributed;
2) targets from the same subject are moderately correlated (r=0.25);
3) results from different arteries can be pooled;
4) the precision of the image analysis tool calculations is 25-75% of the cross-sectional area calculation.

If the SD was 75% of the mean cross-sectional area, then we expect to be able to construct a 95% CI for the bias of half-width of 20% with n=20. Similarly, from Table 8, if the SD was 75% of the mean cross-sectional area, then with n=20, we expect to be able to construct a 95% CI for the precision of 29%.

Table 6: Width of 95% CIs for Bias Based on Total Sample Size (n)*

	n=10	n=20	n=30
SD=6.25 (25%)	±2.42	±1.67	±1.36
SD=12.5 (50%)	±4.84	±3.35	±2.71
SD=18.75 (75%)	±7.26	±5.02	±4.07

*The effective sample size, m, is calculated as m=n×s / [1+(s-1)×0.5]), where s is the number of sections per specimen (=7 in this example). Then the half-width of the 95% CI for bias is $t_{(m-1),\frac{\alpha}{2}}\,(SD/\sqrt{m})$.

Table 7: Estimated 95% CIs for SD Based on Total Sample Size (n)*

	n=10	n=20	n=30
SD=6.25	[4.94,8.51]	[5.27,7.68]	[5.43,7.37]
SD=12.5	[9.88,17.0]	[10.5,15.4]	[10.8,14.7]
SD=18.75	[14.8,25.5]	[15.8,23.0]	[16.3,22.1]

*The effective sample size, m, is calculated as m=n×s / [1+(s-1)×0.5]), where s=7. Then the 95% CI for the

SD is $\left[\sqrt{\frac{(m-1)s^2}{\chi^2_{\frac{\alpha}{2},(m-1)}}}, \sqrt{\frac{(m-1)s^2}{\chi^2_{\left(1-\frac{\alpha}{2}\right),(m-1)}}}\right]$.

4.4.2 DETERMINE MEASURANDS

Import the DICOM files into the analysis software, perform the analysis, and perform steps as required by the Image Analysis Tool to determine tissue characteristics consistent with the requirements set in the Image Analysis activity specification. When evaluating an Imaging Physician, a single tool shall be used for this entire assessment procedure. The assessor shall calculate each cross-section's measurands (Y) (denoted Y_i), where Y denotes the measurand, and *i* denotes the *i*-th target.

4.4.3 CALCULATE STATISTICAL METRICS OF PERFORMANCE

The following shall be performed in a strictly held-out set of subjects and cannot be done iteratively. Once the hold-out set has been used for evaluation, it may not be used for a later assessment after the software changes, except insofar as regression tests are performed where there are no material algorithm changes. It is highly advisable to anticipate this in advance when data is collected and to pre-identify cohorts with sufficient numbers to support potentially many-year development programs.

To properly account for sources of subjectivity, a minimum of three independent pathologist annotations and four positioned-radiologist reader combinations. That is, two independent positionings crossed with two independent radiology readings at each respective position shall be collected and included in the analysis.

To assess bias, plot the value calculated by histopathologic examination versus the value calculated by the Image Analysis Tool. Inspect the resulting plot for associations between the magnitude of the histopathologic measurement and bias, associations between the magnitude of the histopathologic measurements and heteroscedasticity in the image analysis tool measurements, and limits of quantitation of image analysis tool measurements.

To assess linearity, the assessor shall use the NCCLS approach, EP06-A "Evaluation of the linearity of quantitative measurement procedures: A statistical approach; Approved Guideline (2003), of fitting first, second, and third order polynomials and testing that the nonlinear coefficients are near zero. Then estimate the linear slope and provide a 95% CI.

Estimate the precision of the image analysis tool measurements by the standard deviation:

$\sqrt{\frac{1}{n-1}\sum_{i=1}^{n}(Y_i - X_i - \bar{d})^2}$, where $\bar{d}$ is the sample mean of the differences, $\bar{d} = \frac{1}{n}\sum_{i=1}^{n}(Y_i - X_i)$.

Construct a 95% CI for the standard deviation using bootstrap methods.

Present the bias profile (bias of measurements for various ranges of histopathology values versus the histopathology value) and precision profile (standard deviation of image analysis tool measurements from subjects with similar histopathologic values versus the histopathologic value) as summaries of Image Analysis Tool measurement performance for the bias and precision components, respectively. Report the coverage probability at 80% coverage. The coverage probability is the probability that the absolute difference between the value calculated by image analysis tool measurements and the value calculated by histology is less than d0, i.e., $\pi = Pr(|Y - X| < d0)$. Plot the coverage probability for a range of values for d0.

4.5. Assessment Procedure: Multi-parametric Risk Phenotype

This assessment procedure is used by image analysis tool vendors that wish to conform with the Risk Phenotype determination. The relevant performance metrics are weighted kappa, and agreement with expert pathologists, using AUROC by taking each of the three classes as individua two-class problems where the classification problem is the given class vs. either of the two others.

4.5.1 OBTAIN TEST IMAGE SET

Candidate methods need to mitigate the drawbacks of machine learning to keep the benefit of the nonlinearity of the network. One drawback is how relatively few samples can be relied on, given the relative difficulty of obtaining annotated samples in medicine compared to other applications of computer vision, and how to ensure a mechanistic rationale based on biology rather than the algorithm being a black box. These drawbacks are mitigated by using a test set where the input QIBs have been validated and then determining the risk phenotype based on them, rather than raw images, a combination of the individual validated single QIBs, not by any single one. The raw CTA images are not used as model inputs, as raw images are not validated and include excess variability not tied to the actual phenotype that can cause overfitting in models. In summary, the test set must be a strict hold-out from at least two centers, where the single variable QIBs are validated, followed by the multiparametric phenotype classification. The two centers must have at least one statistically significant difference in terms of the variables that pertain to generalizability, such as demographic and/or comorbidities. In cases where either of the centers also contributes training data, a partitioning method utilizing sequential enrollment rather than other partitioning must be used to mitigate overfitting.

When a given section presents with multiple types, only the most clinically significant type shall be used.

Such annotations shall be collected from three pathologists blinded to each other's work.

In order to properly represent the range of expected morphological presentations, the size of the validation set shall be equal to or larger than the sample size required under section 4.4. Figure 2 provides an example distribution of banded types assembled that would meet sample sizing requirements.

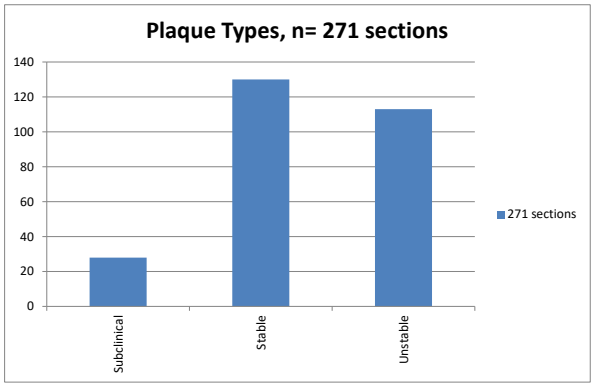

Figure 2: Banded Plaque Type Across All Sections (validation partition, prior to exclusions)

We observe good balance between stable and unstable phenotypes, and as expected, fewer minimal disease sections due to the fact that marginal areas proximal and distal to the plaque that are minimal are not removed surgically. Such a method would meet the requirements under the Profile to extend the set with cross-sections outside of the specimen to achieve balance in the minimal disease. These then raise the number identified in Figure 2.

To assess the degree of agreement among the truthers, we considered for each pair of them, the 3x3

confusion table of their phenotype rating results and calculated the corresponding weighted kappa statistic using the quadratic weights (33).

4.5.2 CALCULATE STATISTICAL METRICS OF PERFORMANCE

Model outputs shall be assessed relative to agreement with an expert pathologist. Under good model development practices, model evaluation was performed on a separate test dataset from that used to develop and train the model. Correctness of classification by the developed model is assessed relative to a consensus panel of pathologists blinded to imaging results. Agreement of classification by the developed model (i.e., classifying as v=1 (minimal, which includes normal), 2 (stable plaque), and 3 (unstable plaque)) with the corresponding truth states (t=1 (minimal), 2 (stable), and 3 (unstable)) will be calculated via the weighted kappa statistic that indicates the proportion of agreement between the assessment categories of two classification results, beyond that expected by chance, penalizing disagreements in terms of their seriousness. The weighted kappa (34, 35), quantified as $\kappa = (p_o - p_e)/(1 - p_e)$, compares the observed agreement $p_o = \sum_{t=1}^{3}\sum_{v=1}^{3} w_{tv}p_{tv}$ with the chance expected agreement $p_e = \sum_{t=1}^{3}\sum_{v=1}^{3} w_{tv}p_{t\bullet}p_{\bullet v}$, where p_{tv}, $p_{t\bullet}$, $p_{\bullet v}$ are the joint and the marginal proportions of the corresponding cross-classification table (Fleiss J., et al., 2013). The weights located at the diagonal represent agreement and thus equal 1. Off diagonal weights indicate the seriousness of disagreement, and the quadratic weighting scheme is given by $w_{tv} = 1 - |t - \nu|^2/4$.

This could be viewed as a cross-section diagnostic biomarker per the NIH BEST definitions.

4.6. Assessment Procedure: Variability of Readers using the Image Analysis Tool

A manufacturer or an imaging site can use this procedure to assess the variability with which the measurands are measured. Variability is evaluated in terms of the repeatability by a single reader and reproducibility by multiple readers. The procedure assesses an Image Analysis Tool and an Imaging Physician operating the tool as a paired system.

Data is provided by the registrant for self-attestation (QIBA Registered) and may be provided by QIBA for a certification program in the future. For each measurand, calculate the intra-reader Standard Deviation (SD) estimated from two or more replicate calculations by the same reader. A minimum of 40 cross-sections from 7 or more subjects per arterial bed are required. Pooling subjects across carotid and coronary arterial beds is only allowable with rigorous statistical justification and, in any case, does not diminish the minimum counts. For each measurand, calculate inter-reader SD estimated from one calculation by two or more different readers. The Reproducibility Coefficient (RDC) shall be estimated as 2.77 $\times$ inter-reader SD. A 95% CI using a chi-square statistic should be used as the pivotal statistic was constructed for the RDC. Minimum counts are as described above for intra-reader variability.

Appendix A: CTA Signal Applicability and Published Performance

The ability of standard CTA to reliably identify atherosclerotic plaque tissue characteristics and correlate them with cardiovascular events relative to the more widely reported use of MRI has not previously been well established in the literature. In principle, the Hounsfield Unit scale used by CT has the potential to be more quantitative than MRI due to the objective basis on which the voxel values are based. Still, terms like "soft plaque" instead of more specific terms like lipid-rich necrotic core are sometimes used in the literature (36), suggesting less specificity. Ideal image processing would take this factor and partial volume effects into account. The speed and high resolution of standard CTA scan protocols promise more widespread adoption. A thorough review paper (37) investigated noninvasive imaging techniques to identify plaque components and morphologic characteristics associated with atherosclerotic plaque vulnerability in carotid and coronary arteries. The review found 62 studies. The 50 studies on the carotid arteries used histology as the reference method. In comparison, the 12 studies on the coronary arteries used IVUS (but this would not be considered definitive as IVUS is itself not validated by histology).

VESSEL STRUCTURE

Source	*Imaging Method*	*Reference*	*object*	*Structure measurement*	*Offset*	*Variability*
de Weert 2006 (38)	CT	Inter-observer	7 Human carotid	Plaque Area (mm2)	-5% constant over 74-111 mm2 range; poor below	8% constant over 74-111 mm2 range; poor below
de Weert 2006 (38)	CT	Inter-observer	13 Human carotid	Lumen Area (mm2)	0% constant over 22-63 mm2 range; poor below	1% constant over 22-63 mm2 range; poor below
Kwee 2009 (39)	CT Auto	1.5T MR	14 Human carotid	Lumen Area	9% constant over 19-72 mm2 range; poor below	37% % constant over 19-72 mm2 range; poor below
Obaid 2013 (40)	CT	Intra-observer	22 Human coronaries	Lumen Area (mm2)	-1% constant over 352-468 mm2 range; poor below	4% constant over 352-468 mm2 range; poor below
Papadopoulou 2013 (41)	CT	Intra-observer	162 Human coronaries	Lumen Area (mm2)	2% constant over 12.8-23.2 mm2 range; poor below	10% constant over 12.8-23.2 mm2 range; poor below
Papadopoulou 2013 (41)	CT	Intra-observer	535 Human coronaries	Vessel Area (mm2)	-1%	7%
Papadopoulou 2012 (42)	CT	Intra-observer	435 Human coronaries	Plaque Area (mm2)	1% constant over 6.1-16.4 mm2 range; poor above	14% constant over 6.1-16.4 mm2 range; poor above
Rinehart 2011 (43)	CT	Inter-observer	85 Human coronaries	Minimum Lumen Diameter (mm)	-2% constant over 1.7-4.4 mm range; poor below	8% constant over 1.7-4.44 mm range; poor below
Rinehart 2011 (43)	CT	Inter-observer	179 Human coronaries	Minimum Lumen Area (mm2)	0% constant over 1.6-21.2 mm2 range; poor below	14% constant over 1.6-21.2 mm2 range; poor below

TISSUE COMPOSITION

With a specific focus on CT, we quote a small illustrative sampling here to indicate the nature and utility of CT for characterizing atherosclerotic plaque:

- (quoted directly from the introduction in (44)) In view of the limitations of [digital subtraction angiography], there is an increasing interest in CTA as a modality for assessing the carotid artery bifurcation. Computed tomography angiography is an imaging modality that can be used to accurately visualize the severity of luminal stenosis in 3D. With CTA it is extremely easy to detect calcifications in the carotid artery. CTA has also become an established method for successful artery calcium scoring in coronary arteries. With the introduction of Multi-detector CT (MDCT) in 1998 fast imaging at high temporal and spatial resolution became possible. … It has been also shown, with comparison to histology, that assessment of carotid atherosclerotic plaque components is feasible with MDCT using different plaque components Hounsfield units (HU) densities in vitro [20] and in vivo [21]. In Figure 1.3 an illustration from of atherosclerotic plaques in MDCT cross-sectional slices and corresponding histology samples are shown.
- (quoted directly from conclusions in (38)) The present study shows that MDCT is capable of characterizing and quantifying plaque burden, calcifications, and fibrous tissue in atherosclerotic

carotid plaque in good correlation with histology, and that lipid core can be adequately quantified in mildly calcified plaques. Furthermore, the MDCT-based assessment of atherosclerotic plaque component quantities was possible with moderate observer variability.

- (quoted directly from conclusions in (45)) Our study results indicate that [dual-source computed tomography] angiography of the carotid arteries is feasible and the evaluation of carotid tissue characteristics allows noninvasive assessment of different plaque components. Although some limitations remain, [dual-source computed tomography] offers a high potential to non-invasively assess the patients at a higher risk for stroke.

An often cited study supporting the use of CT to characterize plaques, while also documenting the factors which can complicate overly simplistic methods (46), states: "The mean CT Hounsfield attenuation was measured for each of the 2x2-mm squares that were electronically drawn on the CT reformatted images and considered in the linear regression model with respect to the percentages of connective tissue, lipid-rich necrotic core, hemorrhage, and calcifications in the corresponding histologic and micro-CT squares. The results of the linear mixed model. Significant overlap was observed in CT Hounsfield densities between lipid-rich necrotic core and connective tissue. There was also some overlap between connective tissue and hemorrhage. Cut-off densities between lipid-rich necrotic core and connective tissue, connective tissue and hemorrhage, and hemorrhage and calcifications were determined as the halfway Hounsfield attenuation between the average densities for each of the components: 39.5 Hounsfield units (HU) between lipid-rich necrotic core and connective tissue, 72.0 HU between connective tissue and hemorrhage, and 177.1 HU between hemorrhage and calcifications."

Wintermark's Table 2, de Weert's result regarding cut-off values (38), and also work by Sieren (47) in lung tissues considered for purposes of establishing the fundamental relationships between tissue types and their HU values generally provide points of comparison with our work. These reference works highlight what is good about using HUs to characterize lesion characteristics, but at the same time, it is challenging. The principal challenge to QIBA-conformant image analysis tool is to mitigate limitations gleaned from the various studies.

More recently, it has been demonstrated that tissue characteristics implicated in high-risk atherosclerotic plaque may be quantitatively measured from routinely available CTA in high correlation with histopathology (22, 48).

Appendix B: Acknowledgements and Attributions

This document is proffered by the Radiological Society of North America (RSNA) QIBA Atherosclerosis Biomarkers Biomarker Committee. The committee is composed of representatives from academia, professional societies, imaging device manufacturers, image analysis image analysis tool developers, image analysis laboratories, biopharmaceutical industry, government research organizations, and regulatory agencies, among others. All work is classified as pre-competitive.

A more detailed description of the committee and its work can be found at the following web link: http://qibawiki.rsna.org/index.php?title=Committees.

QIBA Atherosclerosis Biomarkers Committee Profile Co-Authors:

Abbara, Suhny MD	UT - Southwestern
Buckler, Andrew J. PhD	Elucid Bioimaging Inc.
DeMarco, James Kevin MD	Walter Reed
Dey, Damini PhD	Cedars-Sinai / UCLA
Ferencik, Maros MD, PhD, MCR	Oregon Health & Science University (OHSU)
Jimenez-Juan, Laura MD	University of Toronto, Canada
Kitslaar, Pieter MSc	Medis Cardiovascular Imaging
Kolossváry, Márton PhD	Gottsegen National Cardiovascular Center (Budapest, Hungary)
Konrad, Mathis MSc	University Hospital Heidelberg
Maurovich-Horvat, Pál MD, PhD, MPH, FSCCT, FESC	Semmelweis University (Budapest, Hungary)
Marques, Hugo MD, PhD	Hospital da Luz (Lisbon, Portugal)
Moody, Alan MBBS, FRCP, FRCR	London Health Sciences Centre (Canada)
Moss, Alastair MD, PhD	University of Leicester
Mulshine, James MD	Rush University
Obuchowski, Nancy PhD	Cleveland Clinic Foundation
Paul, Narinder MD, MRCP, FRCR, FRCRC	London Health Sciences Centre (Canada)
Richards, Taylor BS	Duke University
Rinehart, Sarah MD	Piedmont Atlanta Hospital
Saba, Luca MD	University of Cagliari (Italy)
Samei, Ehsan, PhD	Duke University
Schoepf, Uwe Joseph MD	Medical University of South Carolina
St. Pierre, Samantha BS	Elucid Bioimaging Inc.
van Assen, Marly	Univ. Groningen
van Beek, Edwin MD PhD MEd FRCPE FRCR	Edinburgh Imaging
Varga-Szemes, Akos MD, PhD	Medical University of South Carolina
Villines, Todd MD-INMD	University of Virginia
Virmani, Renu, MD	CV Path Institute

QIBA Atherosclerosis Biomarkers Committee Profile Contributors:

Budoff, Matthew MD	Lundquist Institute
Cademartiri, Filippo MD, PhD	SDN IRCCS, Naples, Italy
Carr, Jeffrey MD	Vanderbilt University Medical Center

De Cecco, Carlo MD, PhD	Emory University Hospital
Douglas, Pamela MD	Duke
Duguay, Taylor BS	Medical University of South Carolina | MUSC
Egorova, Svetlana MD, PhD	Elucid Bioimaging Inc.
Ferguson, Terry James MD	Amgen
Ghoshhajra, Brian MD	Massachusetts General Hospital
Guimaraes, Alexander MD, PhD	Oregon Health & Science University
Gupta, Ajay MD	Weill Cornell Medical College
Hall, Timothy PhD	University of Wisconsin
Hanneman, Kate MD	University Health Network, Canada
Hedin, Ulf MD, PhD	Karolinska Institute
Hoelzer, Philipp PhD	Siemens AG Healthcare (Germany)
Hoffman, Udo MD	Massachusetts General Hospital (MGH)
Ikuta, Ichiro MD, MMSc	Yale University School of Medicine
Jackson, Edward F. PhD	University of Wisconsin, School of Medicine & Public Health
Jarecha, Rudresh MBBS, DMRE, DNB	PAREXEL International
Kayaalp-Nalbant, Elif PhD	Illinois Insitute of Technology
Khan, Amir PhD	University of Maryland Medical Center (UMMC)
Krams, Robert MD, PhD	Imperial College London
Lal, Brajesh MD	University of Maryland Medical Center (UMMC)
Narula, Jagat MD, DM, PhD, MACC, FAHA, FRCP	Mt. Sinai School of Medicine
O'Doherty, Jim PhD, MSc	Siemens Healthineers USA, Inc.
O'Donnell, Kevin MASc	Canon Medical Research USA
Perlman, Eric S. MD	Perlman Advisory Group, LLC
Ramirez-Giraldo, Juan Carlos PhD	Siemens Healthineers USA, Inc.
Richards, Toby MD, FRCS	University College London (UCL)
Rossi, Alexia MD, PhD	Erasmus / Circle Cardiovascular
Shaw, Leslee PhD	Mt. Sinai Hospital
Shih, Robert MD	Walter Reed
Siegelman, Jenifer MD, MPH	Takeda Pharmaceuticals
Sullivan, Daniel C. MD	Duke University
Themudo, Raquel MD	Karolinska Institutet
Weintraub, Neil MD	University of Augusta
Williams, Michelle MBChB, PhD, MRCP	University of Edinburgh
Wintermark, Max MD, MAS, MBA	Stanford University Medical Center

The Atherosclerosis Biomarkers Committee is deeply grateful for the support and technical assistance provided by the staff of the RSNA.

References

1. Maroules CD, Hamilton-Craig C, Branch K, Lee J, Cury RC, Maurovich-Horvat P, Rubinshtein R, Thomas D, Williams M, Guo Y. Coronary artery disease reporting and data system (CAD-RADSTM): inter-observer agreement for assessment categories and modifiers. Journal of cardiovascular computed tomography 2018;12(2):125-130.
2. Nadjiri J, Hausleiter J, Jähnichen C, Will A, Hendrich E, Martinoff S, Hadamitzky M. Incremental prognostic value of quantitative plaque assessment in coronary CT angiography during 5 years of follow up. Journal of cardiovascular computed tomography 2016;10(2):97-104.
3. Sullivan DC, Obuchowski NA, Kessler LG, Raunig DL, Gatsonis C, Huang EP, Kondratovich M, McShane LM, Reeves AP, Barboriak DP, Guimaraes AR, Wahl RL, Group R-QMW. Metrology Standards for Quantitative Imaging Biomarkers. Radiology 2015;277(3):813-825. doi: 10.1148/radiol.2015142202
4. Kessler LG, Barnhart HX, Buckler AJ, Choudhury KR, Kondratovich MV, Toledano A, Guimaraes AR, Filice R, Zhang Z, Sullivan DC, Group QTW. The emerging science of quantitative imaging biomarkers terminology and definitions for scientific studies and regulatory submissions. Statistical methods in medical research 2015;24(1):9-26. doi: 10.1177/0962280214537333
5. Raunig DL, McShane LM, Pennello G, Gatsonis C, Carson PL, Voyvodic JT, Wahl RL, Kurland BF, Schwarz AJ, Gonen M, Zahlmann G, Kondratovich MV, O'Donnell K, Petrick N, Cole PE, Garra B, Sullivan DC, Group QTPW. Quantitative imaging biomarkers: a review of statistical methods for technical performance assessment. Statistical methods in medical research 2015;24(1):27-67. doi: 10.1177/0962280214537344
6. Huang EP, Wang XF, Choudhury KR, McShane LM, Gonen M, Ye J, Buckler AJ, Kinahan PE, Reeves AP, Jackson EF, Guimaraes AR, Zahlmann G, Meta-Analysis Working G. Meta-analysis of the technical performance of an imaging procedure: guidelines and statistical methodology. Statistical methods in medical research 2015;24(1):141-174. doi: 10.1177/0962280214537394
7. Obuchowski NA, Reeves AP, Huang EP, Wang XF, Buckler AJ, Kim HJ, Barnhart HX, Jackson EF, Giger ML, Pennello G, Toledano AY, Kalpathy-Cramer J, Apanasovich TV, Kinahan PE, Myers KJ, Goldgof DB, Barboriak DP, Gillies RJ, Schwartz LH, Sullivan DC, Algorithm Comparison Working G. Quantitative imaging biomarkers: a review of statistical methods for computer algorithm comparisons. Statistical methods in medical research 2015;24(1):68-106. doi: 10.1177/0962280214537390
8. Obuchowski NA, Barnhart HX, Buckler AJ, Pennello G, Wang XF, Kalpathy-Cramer J, Kim HJ, Reeves AP, Case Example Working G. Statistical issues in the comparison of quantitative imaging biomarker algorithms using pulmonary nodule volume as an example. Statistical methods in medical research 2015;24(1):107-140. doi: 10.1177/0962280214537392
9. Sigala F, Oikonomou E, Antonopoulos AS, Galyfos G, Tousoulis D. Coronary versus carotid artery plaques. Similarities and differences regarding biomarkers morphology and prognosis. Curr Opin Pharmacol 2018;39:9-18. doi: 10.1016/j.coph.2017.11.010
10. Ibrahimi P, Jashari F, Nicoll R, Bajraktari G, Wester P, Henein MY. Coronary and carotid atherosclerosis: how useful is the imaging? Atherosclerosis 2013;231(2):323-333.
11. Schaar JA, Muller JE, Falk E, Virmani R, Fuster V, Serruys PW, Colombo A, Stefanadis C, Ward Casscells S, Moreno PR, Maseri A, van der Steen AF. Terminology for high-risk and vulnerable coronary artery plaques. Report of a meeting on the vulnerable plaque, June 17 and 18, 2003, Santorini, Greece. European heart journal 2004;25(12):1077-1082. doi: 10.1016/j.ehj.2004.01.002
12. Carter HH, Atkinson CL, Heinonen IH, Haynes A, Robey E, Smith KJ, Ainslie PN, Hoiland RL, Green DJ. Evidence for Shear Stress-Mediated Dilation of the Internal Carotid Artery in Humans. Hypertension 2016;68(5):1217-1224. doi: 10.1161/HYPERTENSIONAHA.116.07698

13. Davies JR, Rudd JHF, Weissberg PL, Narula J. Radionuclide Imaging for the Detection of Inflammation in Vulnerable Plaques. Journal of the American College of Cardiology 2006;47(8, Supplement):C57-C68. doi: http://dx.doi.org/10.1016/j.jacc.2005.11.049
14. Chatzizisis YS, Toutouzas K, Giannopoulos AA, Riga M, Antoniadis AP, Fujinom Y, Mitsouras D, Koutkias VG, Cheimariotis G, Doulaverakis C, Tsampoulatidis I, Chouvarda I, Kompatsiaris I, Nakamura S, Rybicki FJ, Maglaveras N, Tousoulis D, Giannoglou GD. Association of global and local low endothelial shear stress with high-risk plaque using intracoronary 3D optical coherence tomography: Introduction of 'shear stress score'. European heart journal cardiovascular Imaging 2017;18(8):888-897. doi: 10.1093/ehjci/jew134
15. Gnasso A, Irace C, Carallo C, De Franceschi MS, Motti C, Mattioli PL, Pujia A. In vivo association between low wall shear stress and plaque in subjects with asymmetrical carotid atherosclerosis. Stroke; a journal of cerebral circulation 1997;28(5):993-998.
16. Delfino JG, Pennello GA, Barnhart HX, Buckler AJ, Wang X, Huang EP, Raunig DL, Guimaraes AR, Hall TJ, deSouza NM, Obuchowski N. Multiparametric Quantitative Imaging Biomarkers for Phenotype Classification: A Framework for Development and Validation. Acad Radiol 2022. doi: 10.1016/j.acra.2022.09.004
17. Wang X, Pennello G, deSouza NM, Huang EP, Buckler AJ, Barnhart HX, Delfino JG, Raunig DL, Wang L, Guimaraes AR, Hall TJ, Obuchowski NA. Multiparametric Data-driven Imaging Markers: Guidelines for Development, Application and Reporting of Model Outputs in Radiomics. Acad Radiol 2022. doi: 10.1016/j.acra.2022.10.001
18. Kolossváry M, Karády J, Kikuchi Y, Ivanov A, Schlett CL, Lu MT, Foldyna B, Merkely B, Aerts HJ, Hoffmann U, Maurovich-Horvat P. Radiomics versus Visual and Histogram-based Assessment to Identify Atheromatous Lesions at Coronary CT Angiography: An ex Vivo Study. Radiology 2019;293(1):89-96. doi: 10.1148/radiol.2019190407
19. Stary HC. Natural history and histological classification of atherosclerotic lesions: an update. Arteriosclerosis, thrombosis, and vascular biology 2000;20(5):1177-1178.
20. Virmani R, Kolodgie FD, Burke AP, Farb A, Schwartz SM. Lessons from sudden coronary death: a comprehensive morphological classification scheme for atherosclerotic lesions. Arteriosclerosis, thrombosis, and vascular biology 2000;20(5):1262-1275.
21. Virmani R, Burke AP, Farb A, Kolodgie FD. Pathology of the Vulnerable Plaque. JACC 2006;47(8):C13–18.
22. Buckler AJ, Sakamoto A, Pierre SS, Virmani R, Budoff MJ. Virtual pathology: Reaching higher standards for noninvasive CTA tissue characterization capability by using histology as a truth standard. European journal of radiology 2022;159:110686. doi: 10.1016/j.ejrad.2022.110686
23. Buckler AJ, Gotto AM, Jr., Rajeev A, Nicolaou A, Sakamoto A, St Pierre S, Phillips M, Virmani R, Villines TC. Atherosclerosis risk classification with computed tomography angiography: A radiologic-pathologic validation study. Atherosclerosis 2022. doi: 10.1016/j.atherosclerosis.2022.11.013
24. Sullivan DC, Bresolin L, Seto B, Obuchowski NA, Raunig DL, Kessler LG. Introduction to metrology series. Statistical methods in medical research 2015;24(1):3-8.
25. Kessler LG, Barnhart HX, Buckler AJ, Choudhury KR, Kondratovich MV, Toledano A, Guimaraes AR, Filice R, Zhang Z, Sullivan DC, Group QTW. The emerging science of quantitative imaging biomarkers terminology and definitions for scientific studies and regulatory submissions. Statistical methods in medical research 2014. doi: 10.1177/0962280214537333
26. Raunig DL, McShane LM, Pennello G, Gatsonis C, Carson PL, Voyvodic JT, Wahl RL, Kurland BF, Schwarz AJ, Gönen M. Quantitative imaging biomarkers: A review of statistical methods for technical performance assessment. Statistical methods in medical research 2014:0962280214537344.

27. Huang EP, Wang X-F, Choudhury KR, McShane LM, Gönen M, Ye J, Buckler AJ, Kinahan PE, Reeves AP, Jackson EF. Meta-analysis of the technical performance of an imaging procedure: Guidelines and statistical methodology. Statistical methods in medical research 2014:0962280214537394.
28. Obuchowski NA, Reeves AP, Huang EP, Wang XF, Buckler AJ, Kim HJ, Barnhart HX, Jackson EF, Giger ML, Pennello G, Toledano AY, Kalpathy-Cramer J, Apanasovich TV, Kinahan PE, Myers KJ, Goldgof DB, Barboriak DP, Gillies RJ, Schwartz LH, Sullivan DC. Quantitative imaging biomarkers: a review of statistical methods for computer algorithm comparisons. Statistical methods in medical research 2015;24(1):68-106. doi: 10.1177/0962280214537390
29. Obuchowski NA, Barnhart HX, Buckler AJ, Pennello G, Wang X-F, Kalpathy-Cramer J, Kim HJ, Reeves AP, Group CEW. Statistical issues in the comparison of quantitative imaging biomarker algorithms using pulmonary nodule volume as an example. Statistical methods in medical research 2015;24(1):107-140.
30. Tholen DW. Alternative statistical techniques to evaluate linearity. Arch Pathol Lab Med 1992;116(7):746-756.
31. Samei E, Richards T, Segars WP, Daubert MA, Ivanov A, Rubin GD, Douglas PS, Hoffmann U. Task-dependent estimability index to assess the quality of cardiac computed tomography angiography for quantifying coronary stenosis. J Med Imaging (Bellingham) 2021;8(1):013501. doi: 10.1117/1.Jmi.8.1.013501
32. Bae KT. Intravenous contrast medium administration and scan timing at CT: considerations and approaches. Radiology 2010;256(1):32-61. doi: 10.1148/radiol.10090908
33. Agresti A. An Introduction to Categorical Data Analysis. Hoboken, NJ: John Wiley & Sons, Inc., 2007.
34. Goodman LA, Kruskal WH. Measures of Association for Cross Classifications*. Journal of the American Statistical Association 1954;49(268):732-764. doi: 10.1080/01621459.1954.10501231
35. Agresti A. Categorical Data Analysis. 3rd Edition ed, 2013.
36. Naylor AR. Identifying the high-risk carotid plaque. The Journal of Cardiovascular Surgery 2014;55(2):11-20.
37. ten Kate GL, Sijbrands EJ, Staub D, Coll B, ten Cate FJ, Feinstein SB, Schinkel AFL. Noninvasive Imaging of the Vulnerable Atherosclerotic Plaque. Current problems in cardiology 2010;35(11):556-591.
38. de Weert TT, Ouhlous M, Meijering E, Zondervan PE, Hendriks JM, van Sambeek MRHM, Dippel DWJ, van der Lugt A. In Vivo Characterization and Quantification of Atherosclerotic Carotid Plaque Components With Multidetector Computed Tomography and Histopathological Correlation. Arteriosclerosis, thrombosis, and vascular biology 2006;26(10):2366-2372. doi: 10.1161/01.atv.0000240518.90124.57
39. Kwee RM, Teule GJJ, van Oostenbrugge RJ, Mess WH, Prins MH, van der Geest RJ, ter Berg JWM, Franke CL, Korten AGGC, Meems BJ, Hofman PAM, van Engelshoven JMA, Wildberger JE, Kooi ME. Multimodality Imaging of Carotid Artery Plaques: 18F-Fluoro-2-Deoxyglucose Positron Emission Tomography, Computed Tomography, and Magnetic Resonance Imaging. Stroke; a journal of cerebral circulation 2009;40(12):3718-3724. doi: 10.1161/strokeaha.109.564088
40. Obaid DR, Calvert PA, Gopalan D, Parker RA, Hoole SP, West EJ, Goddard M, Rudd JHF, Bennett MR. Atherosclerotic Plaque Composition and Classification Identified by Coronary Computed Tomography: Assessment of Computed Tomography-Generated Plaque Maps Compared With Virtual Histology Intravascular Ultrasound and Histology. Circulation: Cardiovascular Imaging 2013:655-664. doi: 10.1161/CIRCIMAGING.112.000250
41. Papadopoulou S-L, Garcia-Garcia H, Rossi A, Girasis C, Dharampal A, Kitslaar P, Krestin G, de Feyter P. Reproducibility of computed tomography angiography data analysis using semiautomated plaque quantification software: implications for the design of longitudinal studies. Int J Cardiovasc Imaging

2013;29(5):1095-1104. doi: 10.1007/s10554-012-0167-5
42. Papadopoulou S-L, Neefjes LA, Garcia-Garcia HM, Flu W-J, Rossi A, Dharampal AS, Kitslaar PH, Mollet NR, Veldhof S, Nieman K, Stone GW, Serruys PW, Krestin GP, de Feyter PJ. Natural History of Coronary Atherosclerosis by Multislice Computed Tomography. JACC: Cardiovascular Imaging 2012;5(3, Supplement):S28-S37. doi: http://dx.doi.org/10.1016/j.jcmg.2012.01.009
43. Rinehart S, Vazquez G, Qian Z, Murrieta L, Christian K, Voros S. Quantitative measurements of coronary arterial stenosis, plaque geometry, and composition are highly reproducible with a standardized coronary arterial computed tomographic approach in high-quality CT datasets. Journal of Cardiovascular Computed Tomography 2011;5(1):35-43. doi: http://dx.doi.org/10.1016/j.jcct.2010.09.006
44. Vukadinovic D. *Automated Quantification of Atherosclerosis in CTA of Carotid Arteries*: Erasmus University Rotterdam, 2012.
45. Das M, Braunschweig T, Mühlenbruch G, Mahnken AH, Krings T, Langer S, Koeppel T, Jacobs M, Günther RW, Mommertz G. Carotid plaque analysis: comparison of dual-source computed tomography (CT) findings and histopathological correlation. European journal of vascular and endovascular surgery : the official journal of the European Society for Vascular Surgery 2009;38(1):14-19. doi: 10.1016/j.ejvs.2009.03.013
46. Wintermark M, Jawadi SS, Rapp JH, Tihan T, Tong E, Glidden DV, Abedin S, Schaeffer S, Acevedo-Bolton G, Boudignon B, Orwoll B, Pan X, Saloner D. High-Resolution CT Imaging of Carotid Artery Atherosclerotic Plaques. American Journal of Neuroradiology 2008;29(5):875-882. doi: 10.3174/ajnr.A0950
47. Sieren J, Smith A, Thiesse J, Namati E, Hoffman E, Kline J, McLennan G. Exploration of the volumetric composition of human lung cancer nodules in correlated histopathology and computed tomography. Lung Cancer 2011;74(1):61-68.
48. Sheahan M, Ma X, Paik D, Obuchowski NA, St Pierre S, Newman WP, 3rd, Rae G, Perlman ES, Rosol M, Keith JC, Jr., Buckler AJ. Atherosclerotic Plaque Tissue: Noninvasive Quantitative Assessment of Characteristics with Software-aided Measurements from Conventional CT Angiography. Radiology 2018;286(2):622-631. doi: 10.1148/radiol.2017170127